Supporting Information

Cu^{2+} Dual Doped Layer-tunnel Hybrid $Na_{0.6}Mn_{1-x}Cu_xO_2$ as Cathode of Sodium Ion Battery with Enhanced Structure Stability, Electrochemical Property and Air-Stability

Ting-Ru Chen[†], Tian Sheng[‡], Zhen-Guo Wu[*,†,§], Jun-Tao Li[#], En-Hui Wang[†,£], Chun-Jin Wu[†], Hong-Tai Li[†], Xiao-Dong Guo[*†,£], Ben-He Zhong[†], Ling, Huang[§], Shi-Gang Sun[§]

[†]School of Chemical Engineering, Sichuan University, Chengdu, 610065 (PR China);

[‡]College of Chemistry and Materials Science, Anhui Normal University, Wuhu, 241000, P. R. China;

[§]State Key Laboratory of Physical Chemistry of Solid Surfaces, College of Chemistry and Chemical Engineering, Xiamen University, Xiamen, 361005 (PR China).

[#]College of Energy, Xiamen University, Xiamen, 361005 (PR China);

[£]Institute for Superconducting and Electronic Materials, University of Wollongong, Wollongong, NSW 2522 (Australia);

Corresponding Author

* E-mail: zhenguowu@scu.edu.cn (Z.-G. Wu)

[*] E-mail: xiaodong2009@scu.edu.cn (X.-D. Guo)

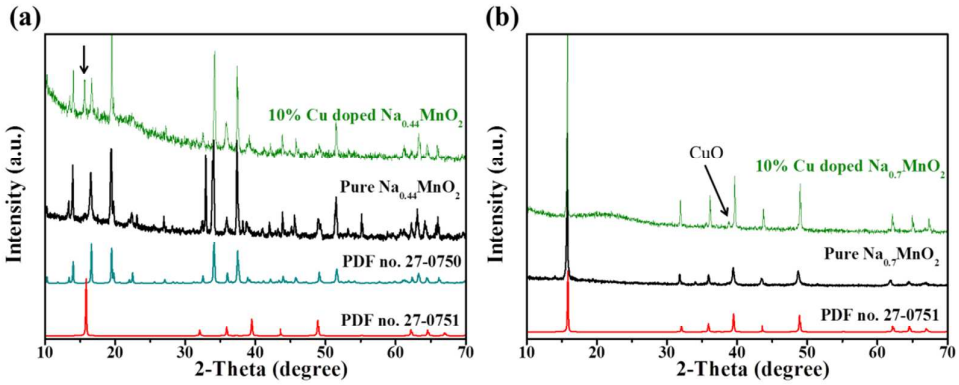

Fig. S1. (a) XRD patterns of pure $Na_{0.44}MnO_2$ and Cu doped sample. (b) XRD patterns of pure $Na_{0.7}MnO_2$ and Cu doped sample.

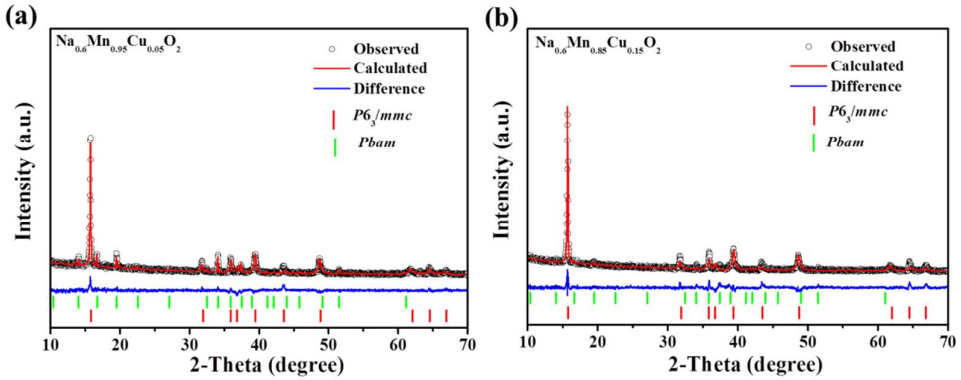

Fig. S2. Rietveld refinement patterns of powder XRD date for layered-tunnel composite structure (a) $Na_{0.6}Mn_{0.95}Cu_{0.05}O_2$ and (b) and $Na_{0.6}Mn_{0.85}Cu_{0.15}O_2$

Table S1. The lattice parameters of various composition of $Na_{0.6}Mn_{0.95}Cu_{0.05}O_2$ and $Na_{0.6}Mn_{0.85}Cu_{0.15}O_2$..

	$Na_{0.6}Mn_{0.95}Cu_{0.05}O_2$		$Na_{0.6}Mn_{0.85}Cu_{0.15}O_2$	
Space group	***P6₃/mmc***	***Pbam***	***P6₃/mmc***	***Pbam***
***a*/Å**	**2.8895**	**9.114**	**2.8912**	**9.097**
***b*/Å**	**2.8895**	**26.317**	**2.8878**	**26.292**
***c*/Å**	**11.280**	**2.8319**	**11.285**	**3.070**
Rp (%)	**6.14**		**6.62**	
Rwp (%)	**8.21**		**9.10**	
χ2	**2.3156**		**3.0161**	
Mass Ratio(%)	**75.4**	**24.6**	**92.8**	**7.2**

Table S2. ICP-OES results of four samples

Theoretical chemical formula	Compositions and ICP-OES results
a:$Na_{0.6}MnO_2$	**$Na_{0.598}MnO_2$**
b:$Na_{0.6}Mn_{0.95}Cu_{0.05}O_2$	**$Na_{0.603}Mn_{0.95}Cu_{0.048}O_2$**
c:$Na_{0.6}Mn_{0.9}Cu_{0.1}O_2$	**$Na_{0.602}Mn_{0.90}Cu_{0.099}O_2$**
d:$Na_{0.6}Mn_{0.85}Cu_{0.15}O_2$	**$Na_{0.604}Mn_{0.85}Cu_{0.148}O_2$**

Table S3. XPS results of four samples

	$Na_{0.6}MnO_2$	$Na_{0.6}Mn_{0.95}Cu_{0.05}O_2$	$Na_{0.6}Mn_{0.9}Cu_{0.1}O_2$	$Na_{0.6}Mn_{0.85}Cu_{0.15}O_2$
Expected Cu state	**N/A**	**+2**	**+2**	**+2**
Expected Mn state	**+3.4**	**+3.47**	**+3.56**	**+3.65**
Mn^{3+}/Mn^{4+}	**1.12**	**0.93**	**0.80**	**0.55**

Table S4. Element content of $Na_{0.6}Mn_{0.9}Cu_{0.1}O_2$ with layered and tunnel structure.

Layered structure			Tunnel structure		
Element	**Weight%**	**Atomic%**	**Element**	**Weight%**	**Atomic%**
O K	**39.61**	**65.04**	**O K**	**22.56**	**47.00**
Na K	**9.72**	**11.11**	**Na K**	**7.52**	**10.91**
Mn K	**44.64**	**21.35**	**Mn K**	**65.96**	**40.01**
Cu K	**6.03**	**2.50**	**Cu K**	**3.96**	**2.08**
Totals	**100.00**		**Totals**	**100.00**	

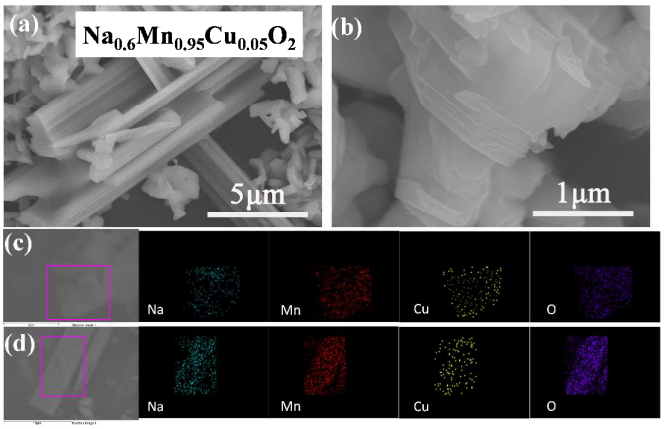

Fig. S3. (a) and (b) SEM images, EDS mapping of $Na_{0.6}Mn_{0.95}Cu_{0.05}O_2$ with plat-like particle (c) and rod-like particle (d), respectively.

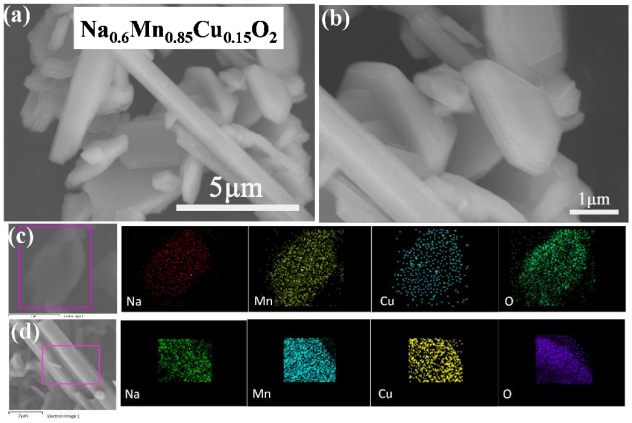

Fig. S4. (a) and (b) SEM images, EDS mapping of $Na_{0.6}Mn_{0.85}Cu_{0.15}O_2$ with plat-like particle (c) and rod-like particle (d), respectively.

Computational methods

All the spin-polarized electronic structure calculations were carried out using the Vienna Ab-initio Simulation Package (VASP) code with Perdew-Burke-Ernzerhof (PBE) functional of exchange-correlation.[1-7] The projector-augmented-wave (PAW) pseudopotentials were utilized to describe the core electron interaction. The on-site Coulomb repulsion correction term (U_{eff} = 4.0 eV) determined by linear response theory was used in the 3d electrons of Mn.[8] The layered $Na_{0.6}MnO_2$ model consists of 24 Na, 36 Mn and 72 O atoms, as shown in Fig. S5a, corresponding to 36 MnO_2 formula unit (f. u.). The tunnel $Na_{0.6}MnO_2$ model consists of 36 Na, 54 Mn and 108 O atoms, corresponding to 54 MnO_2 formula unit (f. u.). The cut-off energy was 450 eV and the Monkhorst-Pack k-point sampling was 2×2×1 for both layered and tunnel $Na_{0.6}MnO_2$. For the Cu doped tunnel $Na_{0.6}MnO_2$, the most stable position for Cu atom are examined at all five different Mn positions, and the most stable position were presented as presented in Fig. S5b.

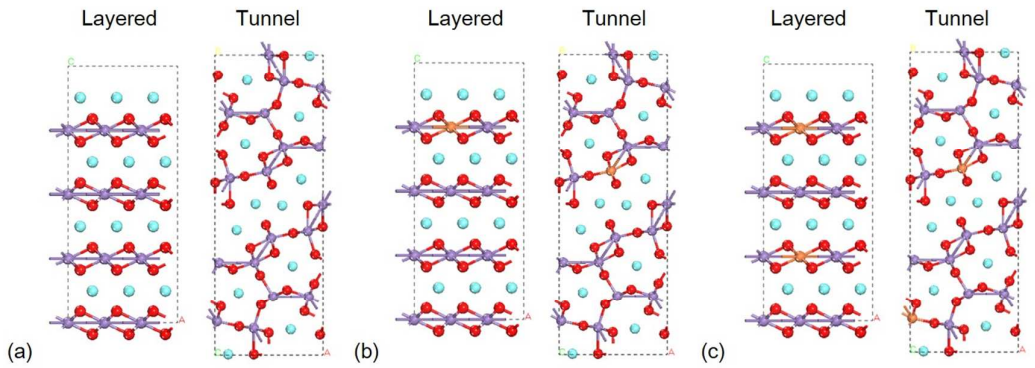

Fig. S5 Theoretical models of (a) pristine, (b) one Cu atom doped, (c) two Cu atoms doped, layered and tunnel $Na_{0.6}MnO_2$ structures. Purple: Mn; red: O; light green: Na; orange: Cu.

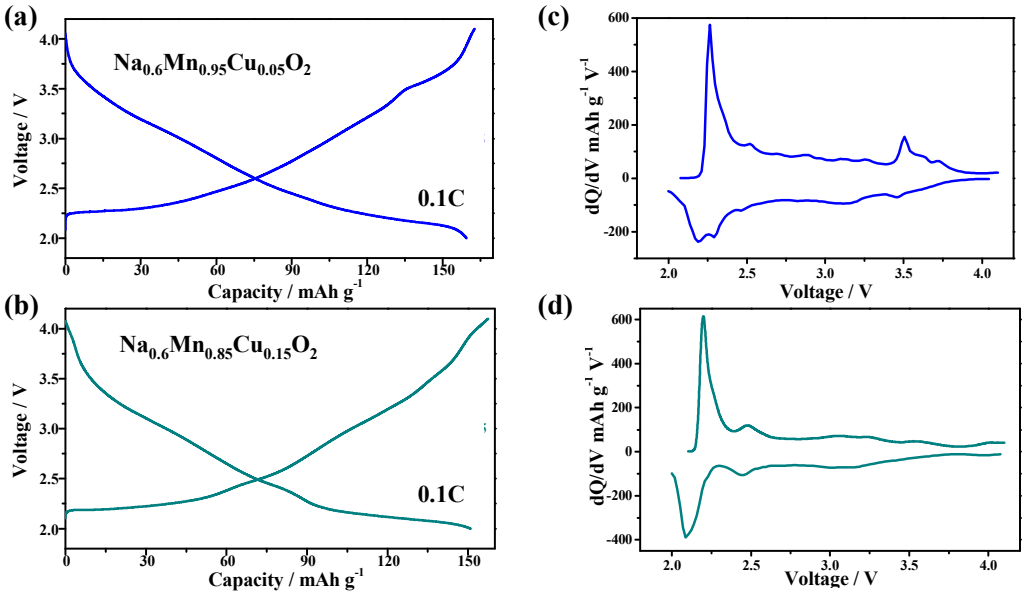

Fig. S6. (a) and (b) The second voltage curves of $Na_{0.6}Mn_{0.95}Cu_{0.05}O_2$ and $Na_{0.6}Mn_{0.85}Cu_{0.15}O_2$ at 0.1C between 2.0 and 4.1V. (c) and (d) Corresponding differential capacity curves of $Na_{0.6}Mn_{0.95}Cu_{0.05}O_2$ and $Na_{0.6}Mn_{0.85}Cu_{0.15}O_2$.

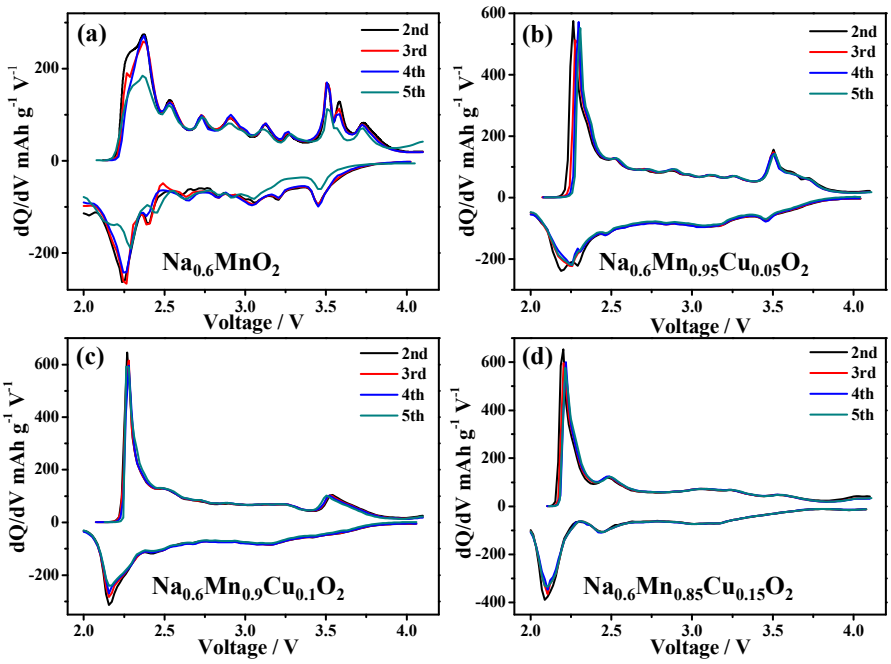

Fig. S7. dQ/dV curves of 2-5 cycles at 0.1C with $Na_{0.6}Mn_{1-x}Cu_xO_2$.(a) x=0; (b) x=0.05; (c) x=0.1 and (d) x=0.15.

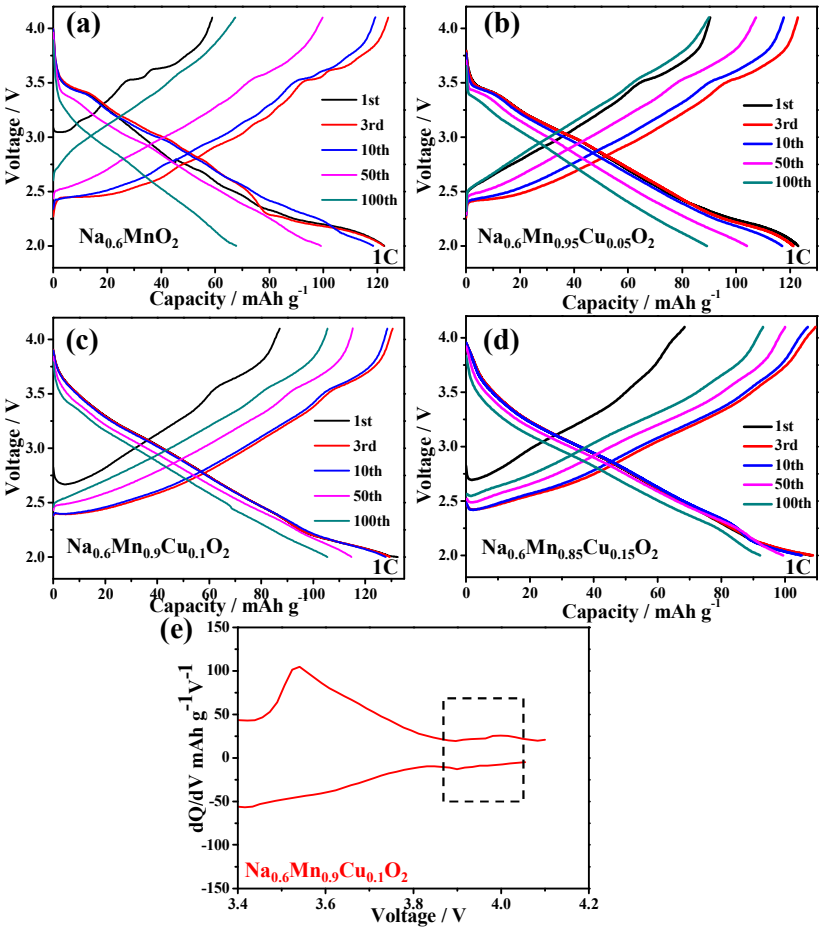

Fig. S8. Charge/discharge curves of (a) $Na_{0.6}MnO_2$, (b) $Na_{0.6}Mn_{0.95}Cu_{0.05}O_2$, (c) $Na_{0.6}Mn_{0.9}Cu_{0.1}O_2$ and (d) $Na_{0.6}Mn_{0.85}Cu_{0.15}O_2$ between 2.0 and 4.1 V at a 1C. (e) Enlarged view of the differential capacity curves of $Na_{0.6}Mn_{0.9}Cu_{0.1}O_2$ at 3.4-4.2V.

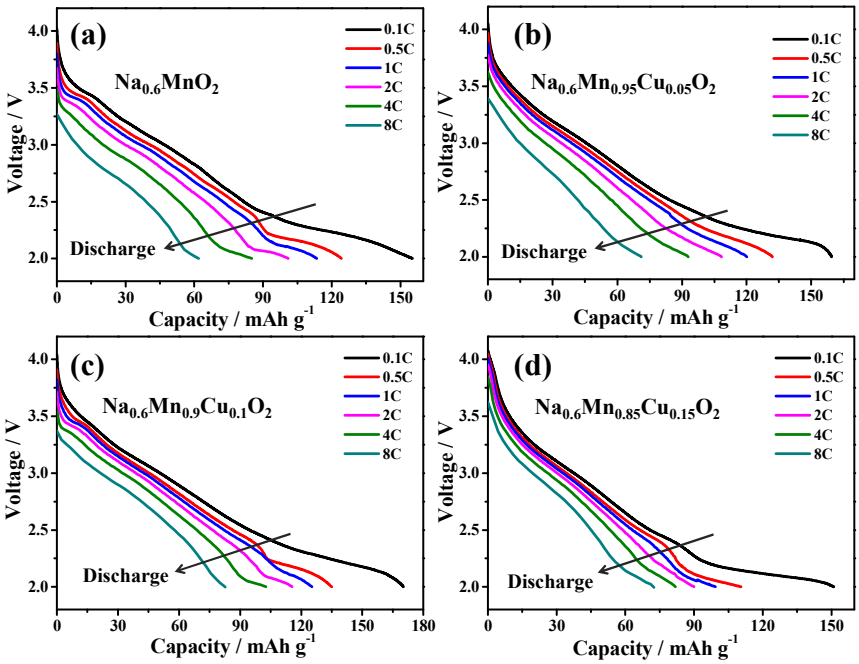

Fig. S9. Discharge curves of (a) $Na_{0.6}MnO_2$, (b) $Na_{0.6}Mn_{0.95}Cu_{0.05}O_2$, (c) $Na_{0.6}Mn_{0.9}Cu_{0.1}O_2$ and (d) $Na_{0.6}Mn_{0.85}Cu_{0.15}O_2$ at various rates.

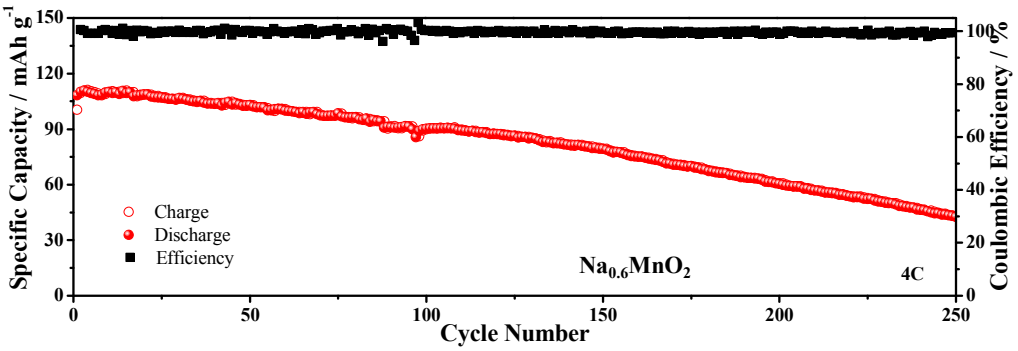

Fig. S10. Long-term cycling performance of $Na_{0.6}MnO_2$ between 2.0 and 4.1V at 4C.

Table S5. The fitting results of equivalent circuit from EIS curves for four samples

sample	R_s / Ω	R_{ct} / Ω	σ	D_{Na} / $cm^2 \bullet s^{-1}$
a: $Na_{0.6}MnO_2$	**5.775**	**288.8**	**287.98**	**4.069×10^{-14}**
b: $Na_{0.6}Mn_{0.95}Cu_{0.05}O_2$	**5.284**	**158.7**	**208.64**	**7.753×10^{-14}**
c: $Na_{0.6}Mn_{0.9}Cu_{0.1}O_2$	**6.440**	**89.3**	**202.52**	**8.229×10^{-14}**
d: $Na_{0.6}Mn_{0.85}Cu_{0.15}O_2$	**6.466**	**351.2**	**304.34**	**3.644×10^{-14}**

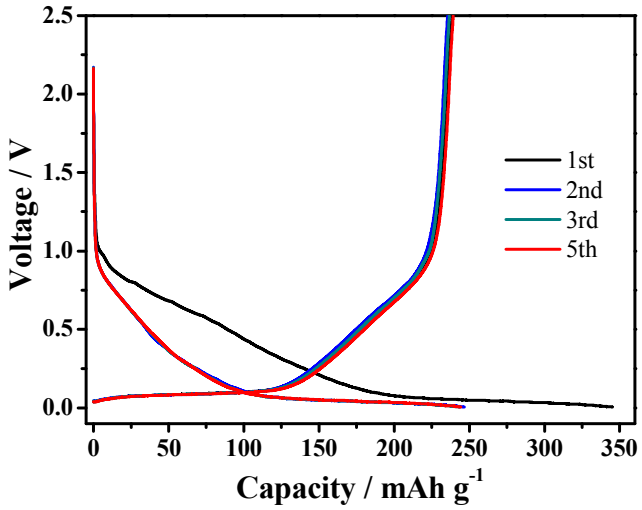

Fig. S11. Charge and discharge curves of hard carbon at 0.1C between 0.005-2.5 V in half cell.

References

1.Kresse, G.; Hafner, J. Ab-Initio Molecular-Dynamics for Open-Shell Transition-Metals. *Phys. Rev. B*. 1993, 48, 13115-13118.

2.Kresse, G.; Furthmuler, J. Efficient Iterative Schemes for Ab-Initio Total-Energy Calculations Using a Plane-Wave Basis Set. *Phys. Rev. B.* 1996, 54, 11169-11186.

3.Blochl, P. E. Projected Augmented-Wave Method. *Phys. Rev. B.* 1994, 50, 17953-17979.

4.Kresse, G.; Joubert, D. From Ultrasoft Pseudopotentials to the Projector Augmented-Wave Method. *Phys. Rev. B.* 1999, 59, 1758-1775.

5. Pedrew, J. P.; Burke, K.; Ernzerhof, M. Generalized Gradient Approximation Made Simple. *Phys. Rev. Lett*. 1996, 77, 3865-3868.

6.Cococcioni, M.; de Gironcoli, S. Linear Response Approach to the Calculation of the Effective Interaction Parameters in the LDA+U Method. *Phys. Rev. B.* 2005, 71, 035105.

7.Franchini, C.; Podloucky, R.; Paier, J.; Marsman, M.; Kresse, G. Ground-State Properties of Multivalent Manganese Oxides: Density Functional and Hybrid Density Functional Calculations. *Phys. Rev. B*. 2007, 75, 195128.